PAPER • OPEN ACCESS

Modification of Corrosion and Mechanical Behaviour of Cu-Zn-Al Shape Memory Alloy

To cite this article: Ali Hubi Haleem *et al* 2021 *J. Phys.: Conf. Ser.* **1973** 012049

View the article online for updates and enhancements.

Modification of Corrosion and Mechanical Behaviour of Cu-Zn-Al Shape Memory Alloy

Ali Hubi Haleem[1], Zuheir Talib Khulief[2], Israa Nayyef Kadhim[3]

[1,2,3] Dept. of Metallurgical Eng., College of Material's Eng., University of Babylon, IRAQ

mat.ali.hobi@uobabylon.edu.iq , mat.zuheir.talib.@uobabylon.edu.iq ,
israa.kadhim.math82@student.uobabylon.edu.iq

Abstract shape memory alloys (SMAs) exhibit an interesting research topic. The current limitation to the SMAs is that the cost of SMAs , made out of expensive elements such as Ni and Ti .In this work, the influence of different amount of nickel (Ni), boron (B), and boron oxide (B_6O) addition on the structure, mechanical , electrochemical, and tribological behaviour of Cu - Zn - Al SMAs have been investigated.

Cu–25Zn–4Al SMAs were produced by powder metallurgy technique with and without the addition of 0.5, 0.7, and 1 wt.% of Ni or B. After mixing the powders for 4hr, the alloys were prepared using 675MPa compact pressure. The alloys were subjected to sintering process in vacuum tube furnace with three steps . For microstructural and phases characterization of alloys with and without the addition of elements (Ni, B), optical microscopy (OM), scanning electron microscopy (SEM), and XRD diffraction analysis were carried out . The transformation temperatures of alloys with and without the addition of elements (Ni, B) were measured by differential scanning calorimetry (DSC). The shape memory properties of alloys with and without the addition of elements (Ni, B) were investigated using shape memory effect test (SME). Electrochemical corrosion tests for alloys with and without the addition of elements (Ni, B) were carried out using potentiodynamic polarization technique. XRD and microstructural analysis showed that all alloys compositions consisted of the predominating Cu_5Zn_8 phase. The results of transformation temperatures showed that the Ni and B additions have strong influences on the transformation temperatures of Cu – Zn – Al SMA .

  The results of electrochemical corrosion tests showed that an increased in Ni or B content up to 1wt. % improved the corrosion resistance of the unmodified Cu – Zn – Al SMA in 3.5 NaCl .   In the second part, the influence of different amount (1,3, and 5 wt. %) of boron oxide (B_6O) additions on the mechanicals and tribology properties of Cu – Zn – Al SMAs with the addition of 1wt.% Ni or 1wt.% B has been investigated.   Hardness measurement was used to assess the mechanical properties of 1, 3, and 5 wt.% B_6O modified Cu – Zn – Al – Ni or Cu – Zn – Al– B alloy compositions. Wet sliding wear process was investigated for 1, 3, and 5 wt.% B_6O modified Cu – Zn – Al – Ni or Cu – Zn – Al – B alloy compositions in distilled water at 2, 5, and 10 N normal load at room temperature. The results of hardness measurements show that an increase in B_6O content up to 3 wt.% improved the hardness of Cu – Zn – Al – Ni and Cu – Zn – Al – B SMAs . The tribological results show that the wear resistance of Cu – Zn – Al – Ni and Cu – Zn – Al – B SMA exhibited the best results with 3 wt. % of B_6O addition. Further increase or decrease of B_6O content decreases the wear resistance of the alloy .

Keywords: Shape Memory Alloy ; Powder Metallurgy; Cu-Zn-Al Alloy; Micro-Hardness ; SMA; Microstructure ;Wear Resistance.

1.   Introduction

Shape memory materials (SMM) are those category of materials which have the memorize or   retain   their previous form when they are subjected to certain stimulus in term of thermal , mechanicals, electrical, chemical, light and magnetic variations. Out of these material SMAs have widely used due to it relatively higher value of specific strength , corrosion resistance , wear resistance , fatigue properties and good actuation response [1] [2].

  The first reported   step   towards the discoveries of the shapes memorys effects SME) were taken in

the 1930s, when a shape memory behaviors was studied in 1932 by ¨ Oleande in his study of ,rubber like effect , in samples of gold-cadmium is ok 1938 by Grainger and Mooradian in his study of brass alloy (copper-zinc). Many year later in 1951 Chang and Read first reported the terms ,shape recovery , Copper, zinc , aluminium alloy are formed between 60% to 80% copper, 15% to 30% consists of zincs, 3% to 10% of aluminium in various proportions. A lamellar structure of metallic Al and brass (Copper-Zinc) foils are introduced for Copper based or aluminums based metals matrixes composite in muffle furnace [3] . In such processes the prepared powder is encapsulated , cold compacted , hot pressed and extruded . However,these 'method are not adapted to all practical requirements and the finished articles often leave something to be desired in their mechanical properties [4] s. The necessary characteristics of these alloys is to ensure the long-time operation of a shape memory alloy . The intermetallic Cu-Zn-Al alloy has been considered for many application as a consequence of low density , high thermal conductivity , high specific modulus , good creep and fatigue resistance [5] [6] .

SMAs are gaining special attention particularly in the aerospace and biomedical applications . A recent well-known project in the aerospace applications of the shape memory alloys involves bending in the variable-geometry chevron (VGC) [7]. In one of the well -developed application , shape memory alloy provide simple and virtually leak proof coupling for pneumatic or hydraulic line [8] . The alloys have also been exploited in mechanical and electromechanical control system , for example a precise mechanical response to small and repeated temperature change . Shape memory alloys are also used in a wide range of medical and dental applications (healing broken bone , misaligned teeth).The various application points of SMA in auto mobiles [9] .

The presented paper focused on analyzing and investigate the effect of Ni and B Additions on Characterization of Cu-Zn-Al SMA alloy prepared by powder metallurgy technique. In order to of improving and developing wear resistance and micro- hardness by adding different weight percentages of elements alloying to Cu-Zn-Al alloy .

2. Experimental work

2.1 Materials and It's Tests

Powders of copper , aluminum , zinc, nickel , boron and boron oxide were used to prepare the alloys. The source of all these powders was Lemandou Ltd. co. China. Basic materials were tested as listed below :

A. Chemical composition analysis for the copper , aluminum zinc , nickel , Boron and boron oxide powders in order to insure their purity. The tests were carried out at General Company for Inspection and Engineering Rehabilitation-Baghdad via Spectro analyzer model (SPECTROMAX) shown in Figure (1).The purity of the powders used are listed in Table (1).

B. Particle size analysis was carried out to all powders using via laser particle size analyzer type : Better size 2000 shown in Figure (2). The tests were carried out at the University of Babylon /College of Materials Eng. . /Ceramics and Building Materials Labs . The average particle size for each used powders is listed in Table (1). The test report of particle size analysis is shown in Figure (2) .

Table (1): The Purity and the Average Particle Size of the Powders Used

Powder	Purity (%)	Average Particles Size (μm)
Copper	99.87	30.62
Zinc	99.75	25.18
Aluminum	99.52	27.8
Nickel	99. 63	31.0
Boron	96.53	35.12
Boron Oxide	98.34	32.43
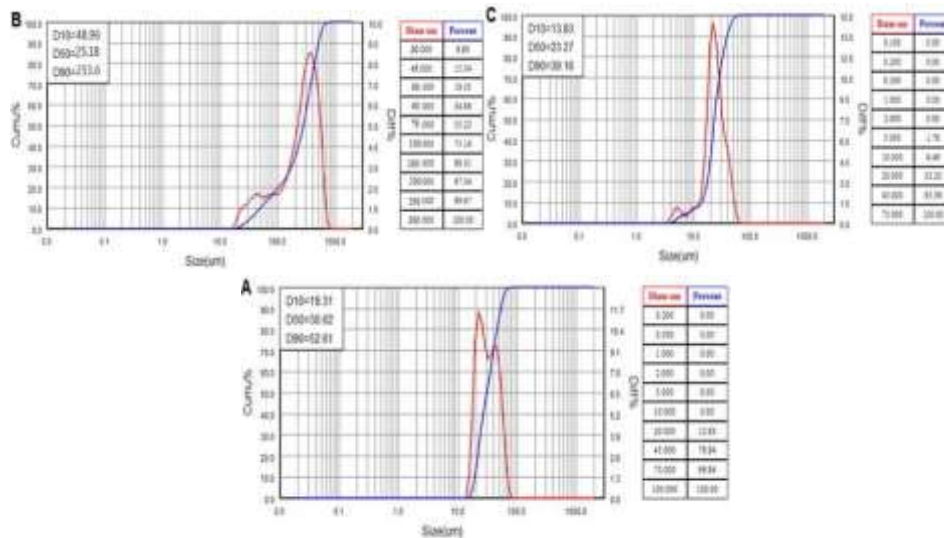
Figure 1: Test Report of Particle Size Analysis; (A) Copper; (B) Zn ; (C)Al

Figure 2: a- The Spectro Analyzer Type (SPECTROMAX) b- Laser particle size analyzer.

2.2 Fabrication of Cu-Zn-Al SMA

Wet mixing for constituents of the mixtures has been done by electrical rolling mixer, original Local. the mixing process was achieved by ball mill, type STGQM -15-2 for 5 hours in order to get the perfect and homogenous distributions of powders particles. Medical alcohol (ethyl alcohol 96%) has been used in wet mixing. The mixture was dried at 60 ^{o}C for 30 min . Chemical Compositions of prepared alloys from elemental powders used in this study have been listed in Table (2).

In this stage, cold uniaxial pressing in double action dies has been used. Compression machines with uniaxial pressing is used to compact green disc samples . Various compacting pressure 675 MPa using double action alloy steel dies fixed in the compression machines with 1800 KN capacity.

Steel die type CT340-CT440 ,was used for the present study as shown in Figure (3) shown the prepared sample . Disc samples with (12.8 mm) in diameter and (6mm) in height used for density, porosity, hardness , optical microscopy , X-Ray diffraction , SEM , shape memory effect, DSC , electrochemical and wet-wear and EDS tests. The inside walls of the steel die were lubricated by graphite .

Table (2) : Mixtures and their Compositions Prepared in this Study.

Alloys	Sample Code	Alloy Compositions wt .%					
		%Cu	%Zn	%Al	%Ni	%B	%B_6O
A	AlloyA	Bal.	25. 029	4.174	----	----	----
B	Alloy B1	Bal.	25.104	4.115	----	0.5	----
	Alloy B2	Bal.	25. 09	4.011	----	0.7	----
	Alloy B3	Bal.	25.107	4.079	----	1.0	----
C	AlloyC1	Bal.	24. 349	4.004	0.5	----	----
	Alloy C2	Bal.	25.122	4.005	0.7	----	----
	AlloyC3	Bal.	24.701	4.015	1.0	----	----
D	AlloyD1	Bal.	25.129	4.017	1.0	----	1
	AlloyD2	Bal.	24. 01	4.103	1.0	----	3
	AlloyD3	Bal.	25.117	4	1.0	----	5
E	AlloyE1	Bal.	24.18	4.303	1.0	----	1
	AlloyE2	Bal.	24. 01	3.973	1.0	----	3
	Alloy E3	Bal.	25.113	4.183	1.0	----	5

Figure 3: a- Types of Prepared Samples, b-Steel Die Used at Present Study.

The sintering process of the green compacts was achieved by vacuum high temperature tube furnace type GSL 1600X shown in Figure (4). A pressure of (10^{-4} torr) was used.The sintering process included the following as shown in Figure (4) :
1.   Heating green compact from room temperature to 350□C.
2.   Soaking time 1hr in 350□C.
3.   Raising the temperature to 550□C.
4.   Soaking time for 2hr at 550□C.
5.   Raising the temperature to 900□C with heating rate 10□C/ min .
6.   Soaking time for 4hr at 900□C.
7.   Slow cooling in furnace.
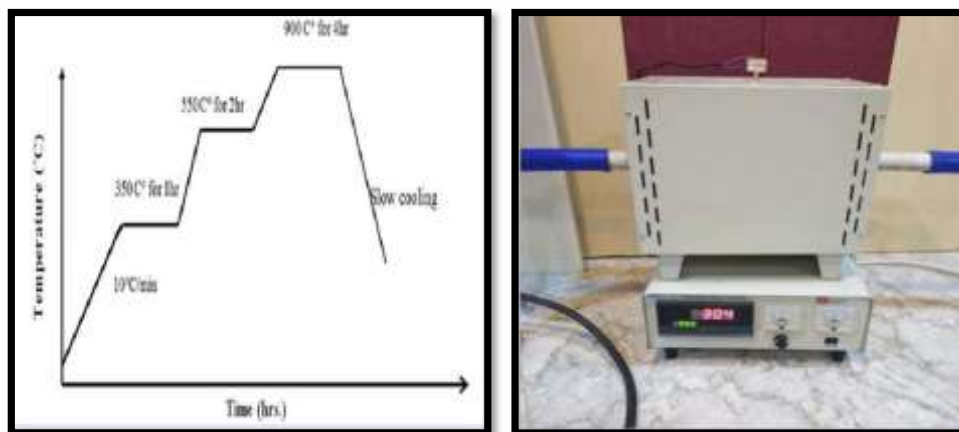
Figure 4: a-The Sintering Program of the Green Sample, b- Vacuum Tube Furnace .

2.3 Optical Microscope Analysis & X-ray Diffraction Analysis (XRD)

Optically microscopes analyses and XRD analyses perform to prepared sintered samples for identify created phases . Optically microscopes analysis carried –out to sintered Cu-Zn-AL shape memory alloys after polish and etch process , using Optically microscopes type : (1270XEQMM310TUSBE). XRD analyses covering the samples via use XRD analyzers types : (Menifee 20) with test situation of:(Target : Cu, wave length of 1.54050A°, voltage and current are 30 KV and 15 mA respectively , scanning speeds of 2deg/min ., and scanning ranges of (20°-80°).

2.4 Micro-Hardness Measurements

The test was carried out using at micro Vickers hardness device type (Digital Micro Vickers Hardness Tester TH 717) using a load of 300g for 10 sec with a square base diamond pyramid. The hardness was recorded as an average of five readings for each specimen.

2.5 Shape Memory Effect Test

Shape memory effect was determined basing on compression test as follows [11]:

$$\text{Shape memory effect (SME \%)} = \frac{d_b - d_a}{d_b} \times 100$$

Where: d_b= diameter of impression in μm before heat treatment.
d_a= diameter of impression in μm after heat treatment.

2.6 Corrosion Test

Corrosion behavior was conducted using the Tafel-Extrapolation .The test was carried out in solution of (3.5gm NaCl +96.5ml distillated water) at room temperature. A platinum wire was used as counter-electrode, the working electrodes were made of cylindrical pieces fastened with appropriate nut and reference electrode . The process has been programmed in computer to draw potential (mv) and log current (μAm) to obtain corrosion current by intersection of the tangent   to the two curves. The corrosion behavior of all alloys has been investigated by Tafel potentiostatic type WENKING M lap shown in Figure (5) that is used to estimate corrosioncurrent and corrosion potential [12].

Figure 5 : Tafel Instruments for Polarizations Test.

2.7 Wet Sliding Wear Test

   Wet sliding wear   was investigated using pin on disk concept using the wet sliding wear device (250 rpm) and constant sliding distance (5mm) with (2,5,10 N) normal load . The lubricants used in the wet-sliding wear tests was distilled water .Shown in Figure (**6**) the sample is weighted before the test using digital electronic balance with four digits . After a period of sliding time (5,10,15, 20, 25 min) , The samples were weight again and the weight loss during sliding wear was measured according toG99-04 ASTM. The relation between weight loss and time is plotted for all alloy to compare the wear behaviour of alloys.

Figure 6: The Wet Sliding Wear device.

3.Result and Discussion

3.1 X -Ray Diffractions & Microscope Analysis

The X-ray peaks for the elements depended on the intensity and theta degree, so that element's data in (intensity -2θ) listed in X-ray data chart. Figure 7 shows the XRD display all phases for reference alloy with 1wt% Ni and with 5 wt. % B$_6$O and reference alloy with 1wt % B and with 5 wt. % B$_6$O after sintering . At this attempt the resulting peaks which indicated after comparing it with standard charts.

Also, It has been shown that the initial stages of homogenization (low temperatures (350 ^{o}C and 550 ^{o}C) first and two stages of sintering) proceed by forming the complete range of compositions from copper and Zinc. This is the manifestation of the initial inter diffusion across the copper- Zinc inter particle boundaries. At later stage of homogenization (high temperature 900 ^{o}C for 4 hours third stage of sintering) result in (βCu$_5$Zn$_8$) intermetallic compound .This results agreement with [13]
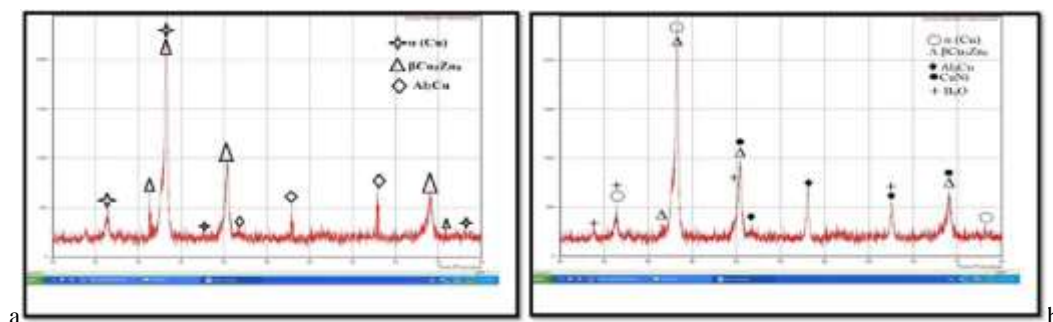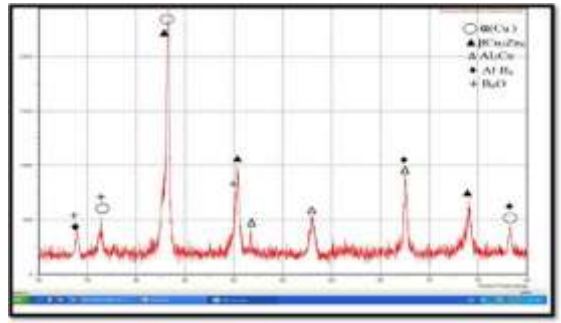
Figure7: **a** XRD Pattern for Sintered Reference Alloy. **b** XRD Pattern for Sintered Reference Alloy with 1wt % Niand with 5 wt. % B_6O . **c** XRD Pattern for Sintered Reference Alloy with 1wt. % B and with 5 wt. % B_6O .

The microstructures of CuZnAl shape memory alloy are shown in Figure 8 observed from images that, the samples after sintering process have a microstructure composed of two regions , light (bright) which represents α-phase network matrix of the microstructure, and the other region is dark which refers to asfine β-phase (intermetallic compound). So, the composition of the Cu-25%Zn-4%Al alloy has α (FCC) + β two- phase region, The microstructure results are in good agreement with X-ray data chart in this present study and specifically matches the structural features reported in [10], [9].
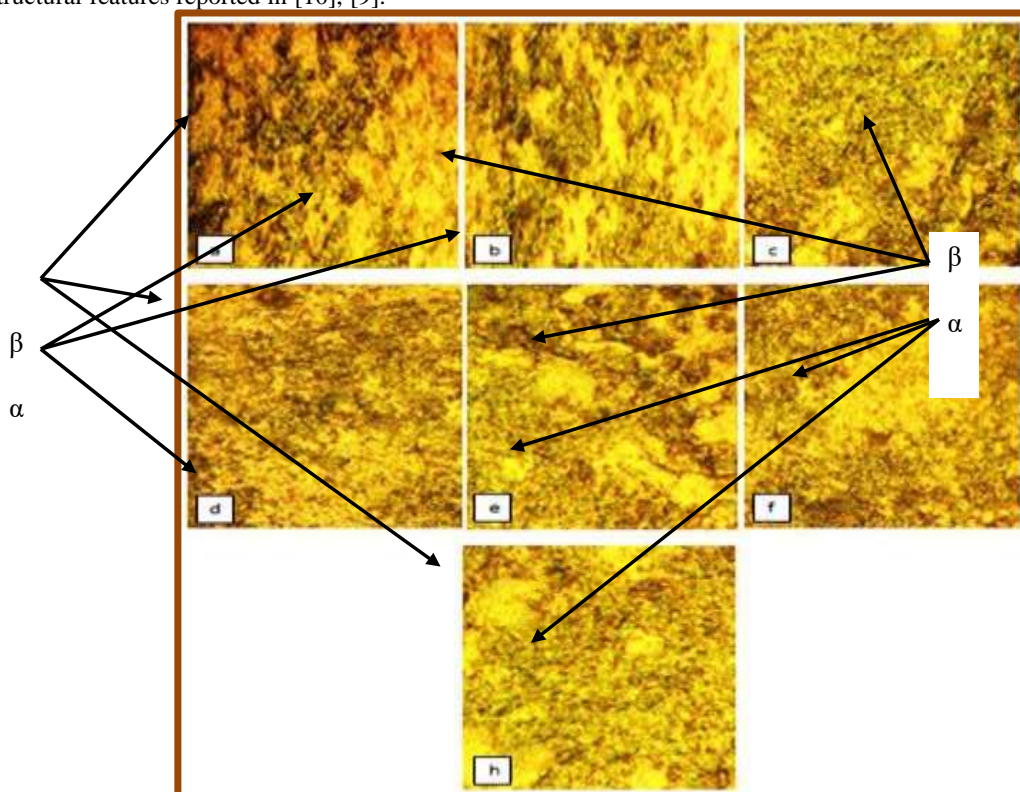
Figure.8 : Optical Microscope Image (600 X): (a) for Sintered Reference Alloy, (b) for Sintered Reference Alloy with 0.5% Ni (c) for Sintered Reference Alloy with 0.7% Ni (d) for Sintered Reference Alloy with 1 wt. % Ni (e) for Sintered Reference Alloy with 0.5% B (f) for Sintered Reference Alloy with 0.7 % B (h) for Sintered Reference Alloy with 1% B (wt.%)

From above images it notice that, an increases at additions of nickel and boron led to a decreases in grain size , because these elements tend to the fine-microstructure [11].

3.2 Scanning Electron Microscopy (SEM) and (EDS)

The mechanical and physical properties of Cu-25Zn-4Al SMAs alloy are significantly affected by the microstructure. So, used Scanning electron microscope (SEM) and energy dispersive spectroscopy (EDS) in orderto examined and identified the microstructures of reference sample (Cu-25Zn-4Al SMA) and samples (base with 5wt. B_6O -1wt. Ni and with 5wt. B_6O - 1 wt. B).Scanning electron microscope images for etched sintering specimens of alloys are shown in Figure (9a-c), Etching reveal grain boundaries which are easily confused with the particle boundaries that also appear as thin gray or black lines [15].
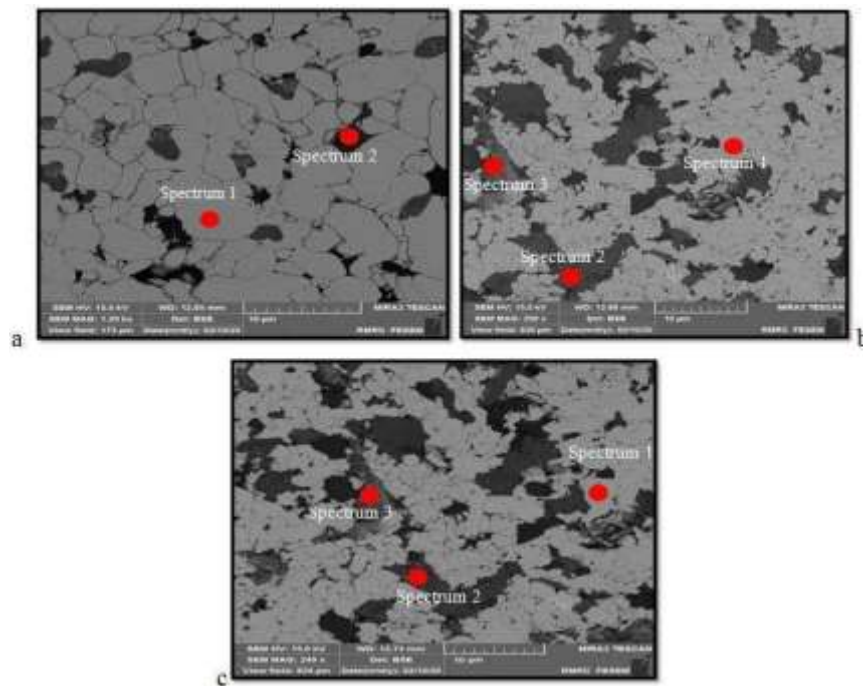
Figure 9:**a** SEM Image for Etched Reference Alloy after Sintering Process **b** SEM image for Reference Alloy with 1% wt of Ni Element with 5wt. B_6O .**c** SEM image for Reference Alloy with 1% wt of B Element with 5wt. B_6O.

While results of Energy dispersive spectroscopy (EDS) that studied and analyzed used to illustrate the chemical composition of the phases and the semi-metallic compounds appearing in the pictures of the base sample and the samples in the presence of the added elements Ni and B with 5%B_6O show in the Figure (10).
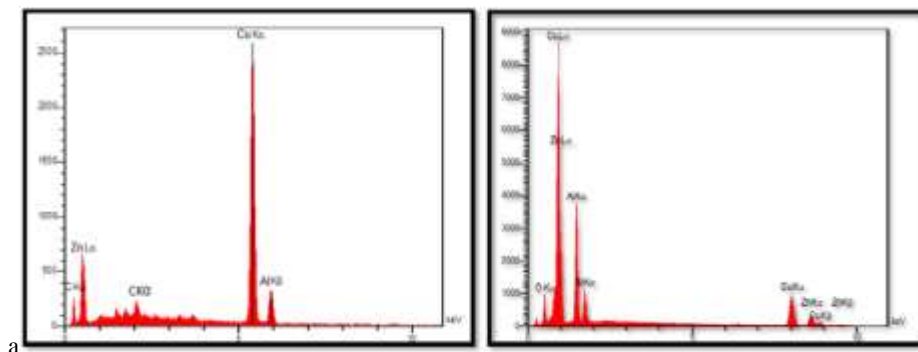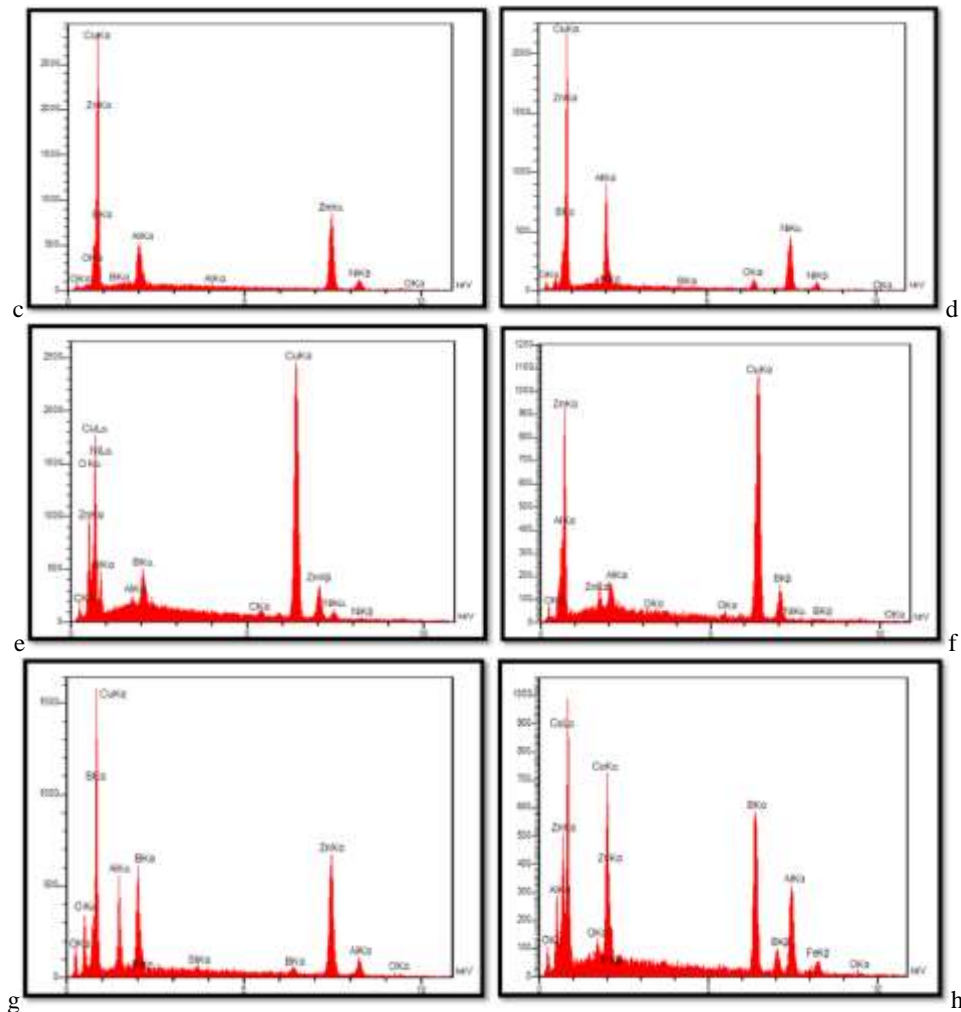
Figure 10:a EDS analysis for reference alloy for Spectrum 1 region .**b** EDS analysis for reference alloy for Spectrum 2 region .**c** EDS analysis for (reference+1%Ni)with 5%B_6O alloy for Spectrum 1 region .**d** EDS analysis for (reference+1%Ni) with 5%B_6O alloy for Spectrum 3 region .**e** EDS analysis for (reference+1%Ni) with 5%B_6O alloy for Spectrum 2 region .**f** EDS analysis for (reference+1%B) with 5%B_6O alloy for Spectrum 1 region .**g** EDS analysis for (reference+1%B) with 5%B_6O alloy for Spectrum 3 region .**h** EDS analysis for (reference+1%B) with 5%B_6O alloy for Spectrum 2 region .

3.3. Differential Scanning Calorimeter (DSC) Analysis

This test is done using DSC series at heating rate of 5 $^oC.min^{-1}$, from 20^oC to 360 ^oC in order to calculate the A_F which is the austenite finish temperature that used in the shape memory effect test as heat treatment temperature. This test has been done for unmodified Cu-Zn-Al alloy and Ni ,B modified Cu-Zn-Al alloy after sintering process as shown in the figures from (11a-c).It was found that the A_S (onset temp.) is 228.32 ℃ and A_F(end set temp.) is 326.26 ℃ for the base alloy(Cu-Zn-Al). When we add 0.5 and 0.7 wt % Ni note that, the transformation temperature is changes , but the maximum of transformation temperature at 1 wt % Ni where the beginning of the transformation temperature from A_S(onset temp.) is 274.64 ℃ to A_F(end set temp.) is 335.38 ℃ as shown Figure (11). The changes of the transformation temperatures take place due to the different type and shape of the austenite phase .
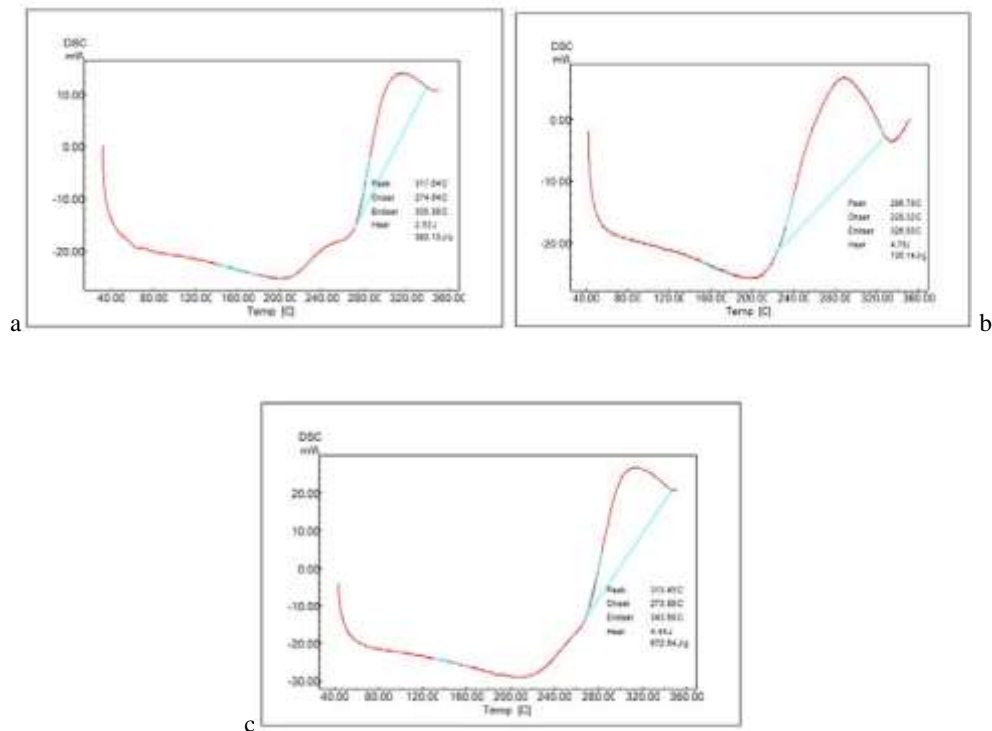
Figure 11: **a** DSC Analysis of Base alloy(Cu-Zn-Al). **b** DSC Analysis For alloy(CuZnAl) with 1 wt % Ni . **c** DSC Analysis For alloy(CuZnAl) with 1wt % B.

3.4 Shape Memory Effect (SME)

The shape memory effect (SME %) all specimens after heat treatment in temperature at more than A_F (end set temp.) with 5 ^{o}C of all specimens. SME% was determined by using Brinell hardness via measuring the diameter of ball indenter after $d_a(\mu m)$ and before $d_b(\mu m)$ the heat treatment. The highest shape memory effect was achieved when the additions was 1 wt% of Ni and B.

The shape memory effect (SME%) of the alloy more than 1 wt% of Ni and B was slight-decrease in SME% because the changes in shape memory effect take place due to appearance the different types the amount of the precipitates and intermetallic compounds might have influence on shape memory effect of the alloy. This agreement with [14]

Table (3) : shape memory effect and shape recovery for alloys.

Alloy No.	Alloy composition	$d_a(\mu m)$	$d_b(\mu m)$	SME%
A	Cu-25n-4Al	485	523	7.26
B1	Cu-25Zn-4Al-0.5 B	551	600	8.16
B2	Cu-25Zn-4Al-0.7 B	485	538	9.85
B3	Cu-25Zn-4Al-1 B	637	721	11.65
C1	Cu-25Zn-4Al-0.5 Ni	577	637	9.41
C2	Cu-25Zn-	420	695.	10.88

	4Al- 0.7 Ni			
C3	Cu-25Zn-4Al-1 Ni	549	627	12.44

3.5 Corrosion Test Results

Electrochemical test for all specimens in 3.5 % NaCl has been done in order to estimate the corrosion rate (mpy) and to investigates the influence of Ni and B on the corrosion resistance of Cu-Zn-Al SMAs.

The corrosion rate (mpy) ,corrosion potential (E_{cor}) and corrosion current density (I_{cor}) of samples calculated from the polarization curve presented in table (4). The corrosion current (I_{corr}) is associated with corrosions rate (mpy) through the following experiential equations.

Notice from the table(4) that, the corrosion rate decreases with increases the percentage weight ratio of the nickel additions to the base alloy from 0. 052 to 0. 03 mpy. So the addition of nickel from 0. 5 to 1 wt has developed and improved the corrosion resistance of Cu-25Zn-4Al alloy by 36% percentage, the reason for this it's that the nickel element addition greatly contributed to the reduction of the grain size this lead to the grain boundaries have increased in a way, which in turn-act as fast passages for the transfer of aluminum ions, which made to form the protective oxides layers and isolates the alloy from the corrosive medium and this decrease in the corrosion rate is attributed to the formation of aluminum oxide (Al_2O_3), cuprous oxides (Cu_2O) and nickel oxides (NiO) layers (as shown in the XRD patterns after corrosion) which act as protective layers on the surface .

Table (4) : Show the Polarization Parameters of Cu–Zn– Al SMA After and Before the Alloying Element Additions in 3.5% NaCl Solution.

Alloy No.	Alloy composition	Corrosion rate C.R (mpy)	Current density I_{corr} (μA/cm)	Corrosion potential E_{corr} (mV)	Corrosion resistance Percentage
A	Cu-25Zn-4Al	0. 0 52	9. 629	-617.4	-----
B1	Cu-25Zn-4Al-0.5 B	0.047	8.324	-1023.8	%9
B2	Cu-25Zn-4Al-0.7 B	0. 043	7.592	-599. 0	%17
B3	Cu-25Zn-4Al-1 B	0.039	7.213	-558. 6	25%
C1	Cu-25Zn-4Al-0.5 Ni	0. 045	8.703	-1012.9	13%
C2	Cu-25Zn-4Al- 0.7 Ni	0. 041	7.962	-1073	21%
C3	Cu-25Zn-4Al-1 Ni	0. 033	6.157	-1038.4	36%

3.5.1 X-Ray Diffraction After Corrosion

In this test X-Ray diffraction for specimens after corrosion test in 3.5% NaCl solution has been done for alloy B3,C3. In Figure (12 a) is the XRD result of alloy B3 , showed that the formation of corrosion products on the specimens surface in 3.5% NaCl solution , the corrosion products were Al_2O_3 , NiO , CuO , ZnO and CuCl. While in the figure(12 b) which is for alloy C3 ,the corrosion products were Al_2O_3 , CuO , ZnO , CuCl and B_2O_3.
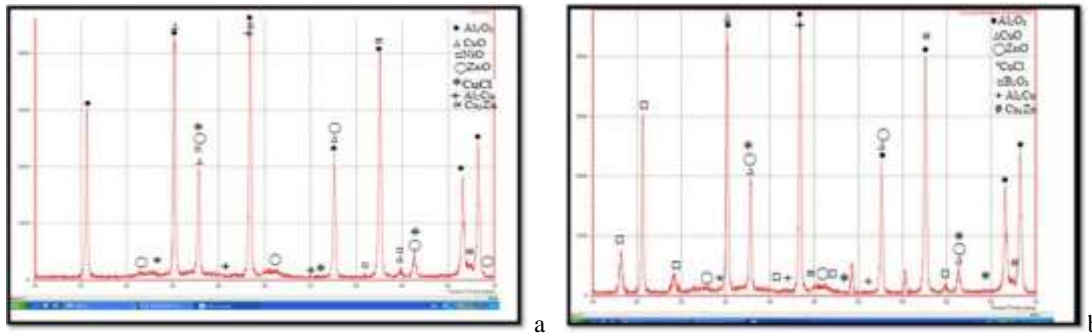
Figure 12:a XRD Analysis For alloy (CuZnAl) with 1 wt % Ni. in(3.5%NaCl solution). **b** XRD Analysis For alloy(CuZnAl) with 1 wt % B. in 3.5%NaCl solution.

3.6 Analysis of Micro-Hardness Results (Hv)

The micro-hardness values for unmodified Cu-Zn-Al alloy and boron oxide modified Cu-Zn-Al alloy are presented in Figure (13). It is observed that the hardness values of the unmodified Cu-Zn-Al alloys are basically increase with increase the boron oxide additions .However, the value of micro hardness slightly decrease with increase the amount of boron oxide up to 5% of both type specimens with Ni and B .This could be related to the increases in boron oxide addition cause decreases on efficiently of sintering processes
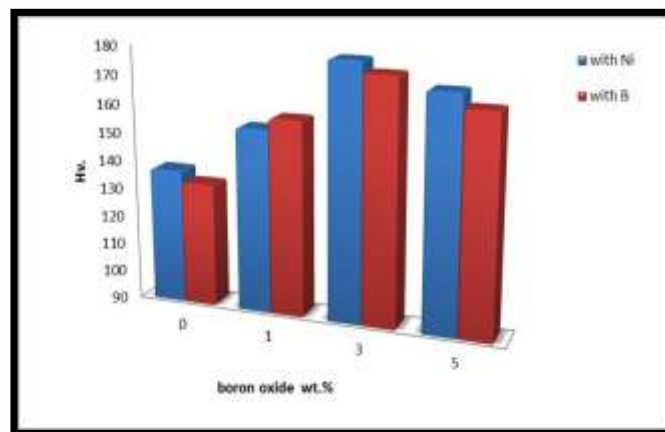
Figure 13 : Hardness for all samples after sintering.

Also, it is seen in Figure (13) most value of the micro-hardness present in samples with Ni addition because this alloying element has been great contribution on finest size grain structure .

3.7 Wet-Sliding Wear Test Results

Disk specimens with (12.8 mm) in diameter and (6 mm) in height have been performed on the specimens of Cu +25 wt% Zn+ 4 wt% Al alloy with and without elements-additions for wet-sliding wear test. The actual mechanisms include material removal due to rubbing action at the interfaces. Loss amount of martial removal

identified of the effect alloying elements in improvement material resistance. The curve of volume loss against time for unmodified Cu-Zn-Al alloy and boron oxide modified Cu-Zn-Al alloy under (2N, 5N and 10N) loads have been presented in Figures 14.

g
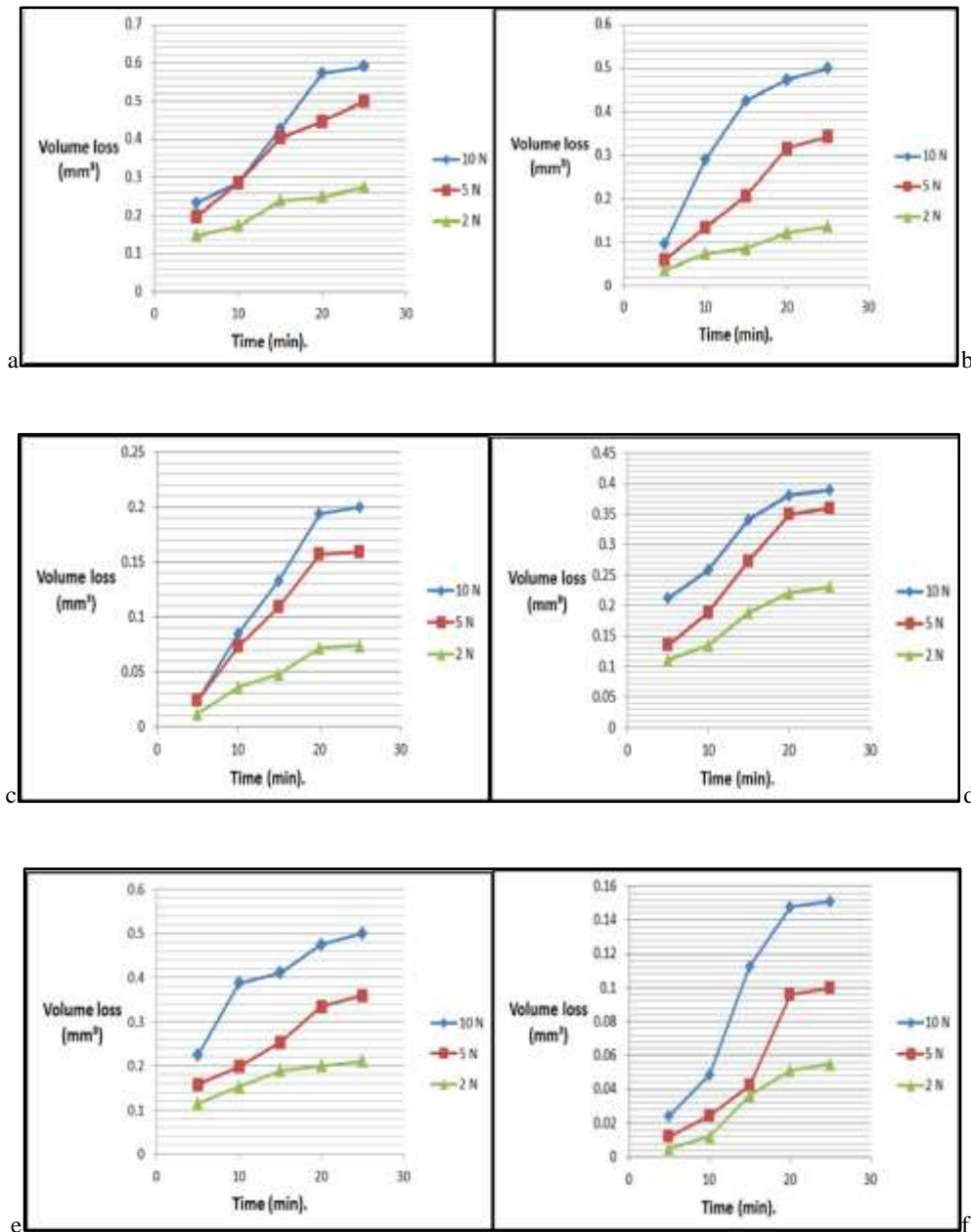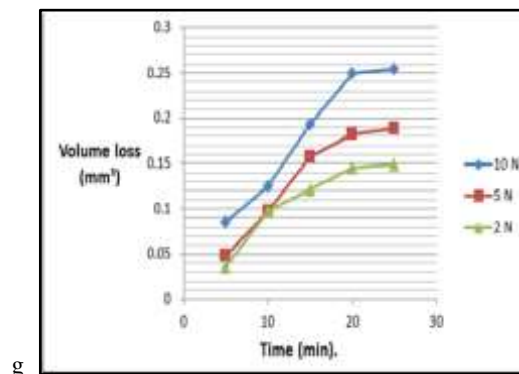
Figure 14 : Volume Loss Vs. Sliding Time for : (a) Sintered Reference Alloy, (b) with 1 wt. % Ni-with 1 wt. % boron oxide, (c) 1wt. % Ni-with 3 wt. % boron oxide, (d) 1wt. % Ni-with 5 wt. % boron oxide, (e) 1wt. % B-with 1 wt. % boron oxide, (f) 1wt. % B-with 3 wt. % boron oxide, (g) 1 wt. % B- with 5 wt. % boron oxide.

It is clear from the Figure   that, the values of volume loss decreased with an increasing the time for all normal loads . The reason is due to the increase in the plastic deformation on the surface of sample exposed to wear , then the removal of material from the surface of this sample. This occurs as a result of overcoming the forces of cohesion and crystalline bonds subjected to friction force between surface of the disc and surface of the specimen caused increased temperature due to an increase in the period of time of the dominated applied load. Furthermore, from the curves, it is identified that wear rate decreases with an increase of the boron oxide content. This could be related to the boron oxide act as the handle and holder of the network-structure of substrate specimens. However wear rate slightly increased at 5 wt.% boron oxide .Thus might be related to may be when increase of the oxide content made decreases in efficiency of the sintering process .

4. Conclusions

The main conclusions from the experimental study of the examined Cu-25Zn-4Al SMA in this research are :

1-   The microstructure of the unmodified Cu-25Zn-4Al alloy and Ni , B and B_6O modified Cu-25Zn-4Al alloy consists of the two phases , α-phase which represent the matrix and β-phase Cu_5Zn_8 which represent the austenite phase .

2-   The Ni and B with modified Cu-25Zn-4Al alloy had austenite transformation temperature value higher than that of the unmodified Cu-25Zn-4Al alloy .

3-   The Ni and B modified Cu-25Zn-4Al alloy show relatively higher SEM compared to the unmodified Cu-25Zn-4Al alloy .

4-   The Ni and B modified Cu-25Zn-4Al alloy show relatively high corrosion resistance compared to the unmodified Cu-25Zn-4Al alloy .

5-   The XRD   results   of the corrosion   product   on the structure of Ni and B modified Cu-25Zn-4Al alloy indicate the position contribution of the Ni and B addition that lead to a denser thicker NiO , B_2O_2 , Al_2o_3 ,CuO , ZnO passive .

6-   The 3wt.% boron-oxide modified Cu-25Zn-4Al-Ni or B alloy had an average hardness value higher than that of unmodified Cu-25Zn-4Al alloy and to other amount of boron oxide used in this study .

7-   The 3wt.% boron-oxide modified Cu-25Zn-4Al-Ni or B alloy show relatively lower   volume loss compared that of unmodified Cu-25Zn-4Al alloy and to other amount of boron oxide used in this study .

References

[1]   Dasgupta R. A look into Cu-based shape memory alloys: Present scenario and future prospects. Journal of Materials Research. 2014;29(16):1681-1698.

[2]   Guerioune M, Amiour Y, Bounour W, Guellati O, Benaldjia A, Amara A, et al. SHS of shape memory CuZnAl alloys. International Journal of Self-Propagating High-Temperature Synthesis. 2008;17(1):41-48.

[3]   Blanco M, Barragan JTC, Barelli N, Noce RD, Fugivara CS, Fernández J, et al. On the electrochemical behavior of Cu-16%Zn-6.5%Al alloy containing the ß'-phase (martensite) in borate buffer. Electrochimica Acta. 2013;107:238-247.

[4]   Ahlers M. Martensite and equilibrium phases in Cu-Zn and Cu-Zn-Al alloys. Progress in Materials Science. 1986;30(3):135-186.

[5]   Jani JM, Leary M, Subic A, Gibson MA. A review of shape memory alloy research, applications and opportunities. Materials and Design (1980-2015). 2014;56:1078-1113.

[6] C. An Hsu, M. Yin Tu, Y. Fu –Hsu and W.H.Wang , The Precipitation Behavior of α1-Plate and γ Phase in Cu-Zn-Sn Shape Memory Alloys, Materials Transactions, 47(9), 2006, 2427 - 2433.

[7] M. H. Wu and L. Mc. Schetky , Industrial application for shape memory alloys : A tutorial review ,proc. Technolgies, Pacific Grove, California, 2000 , 171-182.

[8] W.D.Callister , Materials Science and engineering , 5 th ed .,United States of Amerca ,2000

[9] T. Inaba , N. Shozo , I. Osamu , N.Norihiko and S. Toshihiko, The making of Cu-Zn-Al sintered shape memory alloys , Journal of the Japan Society of Powder and Powder Metallurgy, 36 (2) , 1989, 149-152.

[10] H.W. Kim A study of the two-way shape memory effects in Cu-Zn-Al alloys by the thermo mechanical cyclingmethod J. Mater. Process. Technol., 146 (2004), pp. 326-329

[11] W. Xu. Effects of Gd addition on microstructure and shape memory effect of Cu–Zn–Al alloy J. Alloys Compds., 448 (2008), pp. 331-335.

[12] K.K. Alaneme, E.A. Okotete, M.O. Bodunrin Microstructural analysis and corrosion behaviour of Fe-B modified Cu-Zn-Al shape memory alloys Cor. Rev., 35 (1) (2017), pp. 3-12, 10.1515/corrrev-2016-0053.

[13] T.W. Courtney, Mechanical Behaviour of Materials, second ed., Overseas Press, India, 2006.

[14] Kenneth Kanayo Alaneme and Shaibu Umar, Mechanical behaviour and damping properties of Ni modified CuZnAl shape memory. Journal of Science: Advanced Materials and Devices, 3, (2018), pp. 371-379.

[15] B. M. Rabeeh , M.M EL Batanouny and A. E. EL Ashram , microstructural characterization and solid state processing of Cu-Zn-Al shape memory alloy in a matrix composite , Canadian Journal on Mechanical Sciences and Engineering , 2 (2) , 2011.